Ground-based magnetometer determination of in situ Pc4–5 ULF electric field wave spectra as a function of solar wind speed

I. Jonathan Rae,[1] Ian R. Mann,[1] Kyle R. Murphy,[1] Louis G. Ozeke,[1] David K. Milling,[1] Anthony A. Chan,[2] Scot R. Elkington,[3] and Farideh Honary[4]

Received 7 November 2011; revised 20 January 2012; accepted 23 January 2012; published 24 April 2012.

[1] We present a statistical characterization of ground-based ultra-low-frequency (~1–15 mHz) magnetic wave power spectral densities (PSDs) as a function of latitude (corresponding to dipole L-shells from L~2.5–8), local time, and solar wind speed. We show a clear latitudinal dependence on the PSD profiles, with PSDs increasing monotonically from low- to auroral zone latitudes, where PSDs are peaked before decay in amplitude at higher latitudes. In general, ULF wave powers are highest on the nightside, followed by the local morning, noon, and finally dusk sectors, and are well-characterized and well-ordered by solar wind speed at all MLTs spanning L~2.5–8. A distinct peak in PSD in the 2–8 mHz frequency range above a background power law is evident at most stations studied in this paper, demonstrating a significant non power law like component in the ULF wave power spectrum, in particular at high solar wind speeds. We conclude that field line resonance (FLR) behavior in the magnetosphere is most likely responsible for the peak in PSD, and that such peaks should be included in any radiation belt radial diffusion model addressing radiation belt dynamics. Furthermore, we utilize a model in order to map the ground-based magnetic ULF wave power measurements into electric fields in the equatorial plane of an assumed dipole magnetic field, and find excellent agreement with the in situ CRRES electric fields shown by Brautigam et al. [2005], clearly demonstrating the utility of ground-based measurements in providing reliable estimates of ULF electric field PSD for nowcast input into radiation belt radial diffusion models.

Citation: Rae, I. J., I. R. Mann, K. R. Murphy, L. G. Ozeke, D. K. Milling, A. A. Chan, S. R. Elkington, and F. Honary (2012), Ground-based magnetometer determination of in situ Pc4–5 ULF electric field wave spectra as a function of solar wind speed, *J. Geophys. Res.*, *117*, A04221, doi:10.1029/2011JA017335.

1. Introduction

[2] Enhancements in the flux of relativistic electrons in the Earth's outer radiation belt can cause sudden damage to sensitive spacecraft electronic components, and can pose a health hazard for astronauts [e.g., *Baker*, 2002]. Hence, understanding the energization, transport and loss of relativistic electrons in the Earth's magnetosphere is of importance for satellite operations in the near-Earth space environment. A number of physical mechanisms have been proposed to explain the observed energization, transport and loss of the constituent particle populations of the outer radiation belts (see the review by *Friedel et al.* [2002] for a detailed discussion on this topic), although details of which mechanisms dominate under specific geomagnetic conditions is still not well understood.

[3] The prevailing solar wind speed is related to enhancements in relativistic electron fluxes at geosynchronous orbit [e.g., *Paulikas and Blake*, 1976, 1979], although the relationship appears to be complex [e.g., *Reeves et al.*, 2011]. Furthermore, enhancements in relativistic electron fluxes have also been linked to periods of long-duration ultra-low-frequency (ULF) wave fields in the Pc5 (~2–7 mHz frequencies or 150–600 s period [*Jacobs et al.*, 1964]) wave band in the magnetosphere [e.g., *Rostoker et al.*, 1998; *Baker et al.*, 1998a, 1998b; *Mathie and Mann*, 2000].

[4] ULF wave field line resonances were postulated to exist in the dipole magnetosphere [e.g., *Dungey*, 1955; *Tamao*, 1965] many years before they were observationally verified to exist and contribute to radiation belt dynamics. Strong enhancements in Pc4–5 ULF wave activity have been observed immediately prior to enhancements in the relativistic electron fluxes at geosynchronous orbit during both magnetic clouds [e.g., *Baker et al.*, 1998a, 1998b] and high solar wind speeds [e.g., *Mathie and Mann*, 2001; *Pahud et al.*, 2009; *Huang et al.*, 2010]. During these strong external driving conditions, the magnetospheric cavity may become

[1]Department of Physics, University of Alberta, Edmonton, Alberta, Canada.
[2]Department of Physics and Astronomy, Rice University, Houston, Texas, USA.
[3]Laboratory for Atmospheric and Space Physics, University of Colorado at Boulder, Boulder, Colorado, USA.
[4]Department of Physics, University of Lancaster, Lancaster, UK.

0148-0227/12/2011JA017335

energized via waveguide modes [e.g., *Walker et al.*, 1992; *Samson et al.*, 1992] and extract solar wind energy from magnetosheath flow via Kelvin-Helmholtz activity [e.g., *Hasegawa et al.*, 2004] or over-reflection at the magnetopause [e.g., *Mills et al.*, 1999; *Mann et al.*, 1999]. These waveguide modes can excite long-lasting monochromatic ULF waves in the Pc5 band and if the frequency excited within the waveguide matches the local eigenfrequency of a geomagnetic field line then a standing mode field line resonance (FLR) may be excited [e.g., *Samson et al.*, 1971; *Southwood*, 1974; *Mathie et al.*, 1999; *Mann et al.*, 2002; *Rae et al.*, 2005, 2007; *Lee et al.*, 2007; *Degeling et al.*, 2010]. There further exists a strong correlation between solar wind speed and magnetospheric Pc5 ULF wave power [e.g., *Singer et al.*, 1977; *Rostoker et al.*, 1998; *Mathie and Mann*, 2000, 2001; *O'Brien et al.*, 2001; *Pahud et al.*, 2009]. These observations imply that solar wind speed constitutes one factor controlling Pc5 ULF wave power in the magnetosphere which, in turn, can couple to the large-scale dynamics of energetic electrons in the outer radiation belt. Thus, enhancements in relativistic electron flux, solar wind speeds and Pc4–5 ULF wave power seem to be intimately linked.

[5] One mechanism connecting relativistic electron flux enhancements to ULF wave fields is radial diffusion [see, e.g., *Fälthammar*, 1965]. In general, the radial diffusion coefficients depend on the power spectral density (PSD) of the ULF wave fields in the equatorial plane along electron drift orbits whose frequencies satisfy the drift resonance condition. Theoretical and numerical analyses show that ULF waves can have a significant influence on the energization and dynamics of radiation belt electrons [e.g., *Elkington et al.*, 1999, 2003; *Brizard and Chan*, 2001, 2004; *Hudson et al.*, 2001; *Degeling et al.*, 2007, 2010]. However, in general, it is difficult to prescribe in situ PSD in both local time and L-shell in a region as large as the magnetosphere. Statistical studies of ULF wave power in the magnetosphere have been completed at specific L-shells (e.g., at geosynchronous orbit [*Huang et al.*, 2010]) or across a wide range of L-shells and local times but only for short epochs (e.g., with CRRES [*Brautigam et al.*, 2005]). In addition, very few case studies have been able to determine the ULF fluctuation spectrum in both the azimuthal electric and compressional magnetic fields concurrently [e.g., *Sarris et al.*, 2009]. Both of these fields are thought to contribute to radial diffusion, however observations of both fields simultaneously are in general limited to point-measurements at specific L-shells and specific local times.

[6] In this paper, we present the basis of an alternate approach which uses ground-based magnetometer data to overcome the lack of in situ coverage. We use ~15 years of ground-based magnetometer data to calculate ground-based PSD as a function of L-shell, local time and solar wind velocity. Using an Alfvénic model of the magnetic and electric field structure along geomagnetic field lines we infer the corresponding electric field PSDs in the equatorial magnetosphere (see *Ozeke et al.* [2012] for details) and compare our estimates to the electric fields observed in space by *Brautigam et al.* [2005]. We find excellent agreement between the statistics of the electric fields derived from the ground-based data and the statistical PSDs of transverse electric field power presented by *Brautigam et al.* [2005] over a wide range of L-shells. This suggests that ground-based measurements can provide an excellent proxy for estimating equatorial electric fields over a wide range of L-shells, local times and solar wind conditions.

[7] In a companion paper [*Ozeke et al.*, 2012], we detail an extension of the results obtained in this study by averaging the dayside ground-based ULF wave power and hence the equatorial electric field PSD in order to calculate the resultant electric diffusion coefficient, D_{LL}^{E}, and compare with diffusion rates obtained by *Brautigam et al.* [2005] and with the empirical diffusion coefficients derived by *Brautigam and Albert* [2000]. We find good agreement between the ground-based determination of equatorial electric fields and those observed by CRRES, demonstrating that ground-based magnetometer measurements can be utilized to predict the ULF wave fields in space with reasonable accuracy.

2. Data and Methodology

[8] We use approximately fifteen years of data from four selected ground-based magnetometer stations from the CANOPUS (Canadian Auroral Network for the OPEN Program Unified Study [*Rostoker et al.* [1995]), now operated as the Canadian Array for Real-time Investigations of Magnetic Activity (CARISMA) [*Mann et al.*, 2008]) fluxgate magnetometer array from January 1990 to May 2005 at 5 s cadence. These four magnetometer stations lie along the "Churchill Line" meridian, and correspond to L-shells that approximately span the outer radiation belt region from L~4–8. We further extend the CANOPUS/CARISMA "Churchill Line" coverage to lower L-values with data from two magnetometer stations from the European sector SAMNET (Sub-Auroral Magnetometer NETwork [e.g., *Yeoman et al.*, 1990] http://www.dcs.lancs.ac.uk/iono/samnet/) array over a similar 15-year period (1987–2002 inclusive). Table 1 shows the station locations in geographic and geomagnetic coordinates, as well as the L-shell and the period of data used in this statistical study. The range of geomagnetic station positions reflects changes due to the IGRF in the time interval studied in the paper.

[9] Hourly estimates of the ULF wave power spectral density (PSD) are computed in both the magnetic H- and D-components, which correspond to the local geomagnetic north-south and east-west magnetic perturbations observed on the ground. Each hourly time series has a mean removed and Hanning window applied. Note that any section of any hourly time series with a data gap, data spike or otherwise erroneous data point is discarded. The windowed time series is then transformed from the time to the frequency domain via equation

$$F_k = \sum_{n=0}^{N-1} x_n w_n \exp\left[\frac{-2\pi i k n}{N}\right] \quad (1)$$

where x_n denotes the time series, w_n denotes the windowing function, and N is the length of each series. The power spectral density of each hourly window is then calculated from:

$$PSD_k = \frac{1}{\Delta f W} 2\left|F_k\right|^2 \quad (2)$$

Table 1. The Six Stations Used in This Study, Together With Their Station Code, Geographic and Corrected Geomagnetic Latitudes and Longitudes[a]

		Geographic		Corrected Geomagnetic			
Station	Code	Latitude (deg)	Longitude (deg)	Latitude (deg)	Longitude (deg)	L Shell and Ranges	Data Interval Used and Central Year
Fort Churchill	FCHU	58.76	265.91	69.04 (69.36–68.63)	331.81 (330.76–332.81)	7.94 (8.18–7.65)	1997 (1990–2004)
Gillam	GILL	56.38	265.36	66.73 (67.04–66.33)	331.41(330.41–332.36)	6.51 (6.68–6.30)	1997 (1990–2004)
Island Lake	ISLL	53.86	265.34	64.31 (64.60–63.92)	331.83 (330.89–332.73)	5.40 (5.52–5.26)	1997 (1990–2004)
Pinawa	PINA	50.20	263.96	60.60 (60.86–60.24)	330.27 (329.39–331.11)	4.21 (4.28–4.12)	1997 (1990–2004)
Glenmore Lodge	GML	57.16	3.68	54.31 (54.37–54.26)	84.13 (84.41–83.56)	2.98 (2.99–2.98)	1994 (1987–2002)
York	YOR	53.95	1.05	50.83 (50.93–50.73)	80.73 (80.98–80.20)	2.55 (2.56–2.54)	1994 (1987–2002)

[a]Values are shown with the middle year of the study, and the range of values shown in parentheses.

where Δf is the frequency resolution defined $\Delta f = 1/N\Delta t$ for a series of length N sampled at a resolution of Δt, and W is a normalization constant for the windowing of the hourly time series defined by

$$W = N \sum_{n=0}^{N-1} w_n^2.$$

Finally, each hourly PSD is assigned an observed solar wind velocity and Kp value according to the OMNI database (http://nssdcftp.gsfc.nasa.gov/spacecraft_data/omni/).

[10] This method of calculating PSD is equivalent to the method used by *Brautigam et al.* [2005], and produces window length-independent estimates of PSD. The hourly median PSD as a function of frequency and MLT was calculated for each of the 7 ground stations and collated into solar wind speed bins of <300, 300–400, 400–500, 500–600, 600–700 and >700 km/s. This database has already been utilized to compute the summed Pc5 ULF wave power in the 1–10 mHz and 2–10 mHz bands as a function of MLT and v_{sw} (see *Pahud et al.* [2009] for details) and to examine the dependence of Pc5 power spectra on solar cycle phase and solar F10.7 flux (see *Murphy et al.* [2011] for details). Finally, we also compute an hourly median PSD as a function of Kp for a specific comparison to the fits to PSD as a function of Kp using in situ CRRES data as detailed by *Brautigam et al.* [2005].

[11] In order to simplify the presentation of the results, we combine individual hours of MLT into four local time regions centered on 6, 12, 18 and 24 MLT; that is, for a given 6-h MLT sector, we determine a PSD that is characteristic of each of the dawn, noon, dusk and midnight local time sectors by calculating the mean of the six individual median PSD estimates calculated independently for each of the 6 one-hour MLT data windows for each station.

[12] In order to compare these ground-based power estimates to previous statistical studies using in situ satellite data we map the ground-based PSD estimates into equatorial electric field PSDs using the expression in equation (3) and *Ozeke et al.* [2012]

$$PSD_{eq}^{E} = \left[\frac{E_{eq}}{b_g}\right]^2 PSD_g^b \qquad (3)$$

where E_{eq}/b_g is the ratio of equatorial electric field to ground-based magnetic field for the Alfvénic eigenfunctions of the *Ozeke et al.* [2009] model. This implies that the electric field PSD_{eq}^{E} in the equatorial plane can be determined from the magnetic field PSD_g^b measured by the ground-based magnetometers, and that this ratio is proportional to the square of the wave frequency since the ratio E_{eq}/b_g is proportional to frequency [see *Ozeke et al.*, 2009, equations (23) and (24)]. This in turn means that the gradient of the PSD_{eq}^{E} as a function of frequency is different from that of the PSD_g^b as a function of frequency. For example, an observed plateau in the PSD_g^b will in fact produce a positive gradient in PSD_{eq}^{E}.

3. Results

[13] Figure 1 shows the variation of ground-based magnetic ULF PSD in the H- and D-components as a function of MLT and solar wind speed for the GILL magnetometer station, which is at a median location of L = 6.51 during the period of study. It is clear from Figure 1 that there is a well-ordered solar wind speed dependence of ULF wave PSD in both the H- and D-components in each of the four local time sectors. In each of these four MLT sectors, the median ULF wave PSD increases monotonically with increasing solar wind speed at all frequencies over the studied frequency range from 0.7 to 15 mHz. The PSD in all four local time sectors can be well-described either as a simple power law like power spectrum, or as a power law spectrum with an additional superposed localized Gaussian power enhancement above the power law centered at a specific frequency (hereafter termed as a "Gaussian enhancement" for brevity). The PSDs that can be described only by a power law can be most easily seen in the midnight sector, where the PSD profiles are close to linear on this log-log scaled plot. The power law plus Gaussian enhancement PSDs are most obviously in the dawn and noon sectors at high solar wind speeds, but are also obvious in the dusk sector at both high and low v_{sw}. Finally, in general the H-component PSDs are slightly larger than the D-component PSD at each frequency in each MLT sector, and the PSDs are larger in the dawn sector than those seen at dusk. For brevity, in the supplementary material, we include the ground-based PSDs from the other five magnetometers used in this study (FCHU, ISLL, PINA, GML and YOR).

[14] Ground-based magnetic PSDs are mapped to equatorial electric fields using equation 3. The conversion factor for mapping the ground magnetic field PSD_g^b to the electric field PSD_{eq}^{E} in the equatorial plane is a function of the latitudinal spatial scale of the wave $\Delta\theta$ and the azimuthal wave number m [cf. *Ozeke et al.*, 2009]. In these studies, we use $\Delta\theta = 4^\circ$ and select a single value of m = 1 for simplicity,

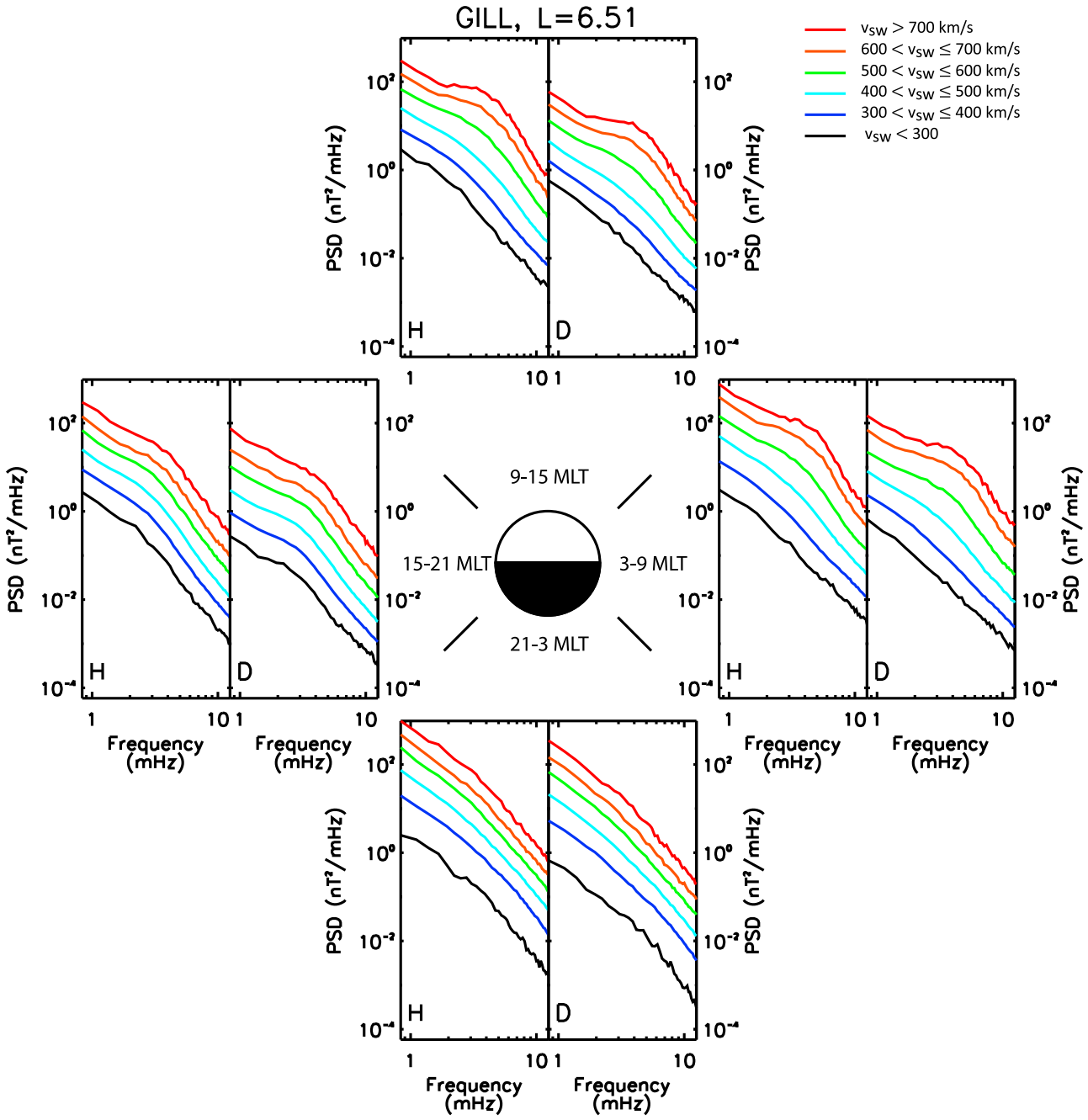

Figure 1. Ground-based median magnetic ULF wave power spectral density (PSD) as a function of magnetic local time (MLT) and solar wind speed for the GILL magnetometer station (L ~ 6.51). Each two-plot section displays the ground-based magnetic PSD in four different MLT sectors corresponding to dawn (3–9 MLT, right), noon (9–15 MLT, top), dusk (15–21 MLT, left) and midnight (21–3 MLT, bottom). In each MLT sector, the left-hand plot displays the MLT sector averaged median H-component PSD (the mean of the median PSD calculated independently for each of the 6 UT hours of data in this MLT sector), and the right-hand plot shows the MLT sector averaged median D-component PSD, as a function of solar wind speed.

though in reality these numbers will not be constant from day-to-day nor necessarily across all ULF frequencies studied in this paper. However, we do note that changing the value of m does not have a strong effect on the mapped electric field PSD^{E}_{eq} value. For example increasing the value of m from 1 to 20 increases the electric field PSD^{E}_{eq} by less than a factor of 2.7.

[15] Figure 2 shows the mapped electric field PSDs in the radial (Er) and azimuthal (Eφ) directions obtained from the *Ozeke et al.* [2009] mapping, in the same format as described

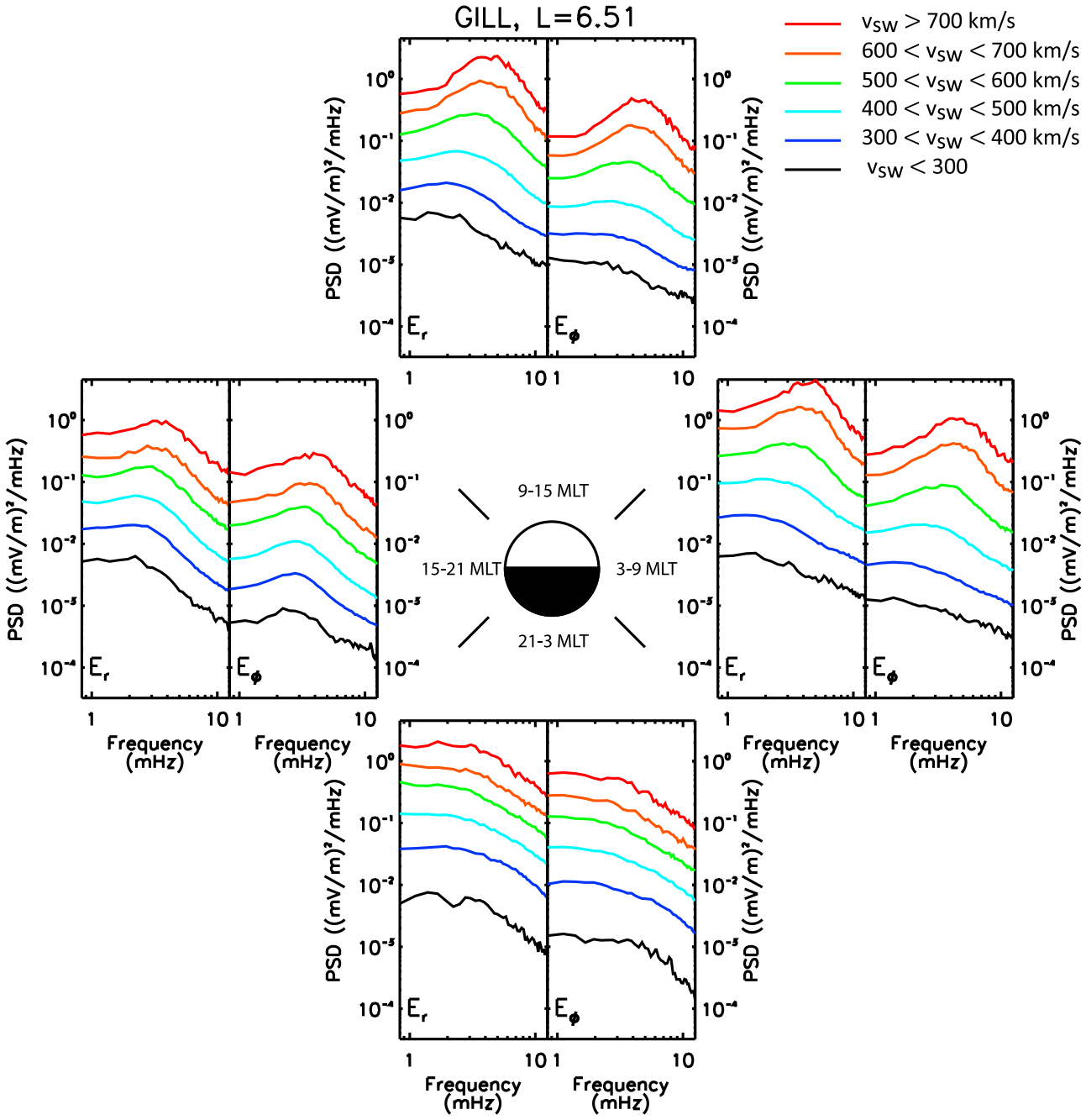

Figure 2. Mapped ULF wave electric field PSD derived from the GILL magnetometer station as a function of MLT and solar wind speed, for (left) radial Er and (right) azimuthal Eφ components in the same format as Figure 1, and using the model outlined by *Ozeke et al.* [2009, 2012].

in Figure 1, for the GILL magnetometer. Note that a perfect 90° rotation from an Alfvénic eigenmode on transmission through the ionosphere has been assumed. In this case, the H- and D-components on the ground map to the toroidal mode Er and poloidal mode Eφ in the magnetosphere, respectively. In general, the mapped Er is larger than the Eφ component, which is clearest in the noon sector. Also clear from Figure 2 is that the "power law plus Gaussian enhancement" PSD translates to a clear peak in PSD in equatorial electric fields, Er and Eφ, as a function of frequency for the majority of solar wind speeds and local times. The power law part of the power spectrum is also shallower than its ground-based counterpart, as expected from the mapping. Interestingly, the peak PSD tends to occur at slightly higher frequencies for higher v_{sw} values. Further, although the peaks in PSD are larger in Er than Eφ at most local times, peaks in PSD clearly occur in both electric field components. Finally, the ULF wave PSD at midnight can no longer be described primarily as a power law spectrum with a single index, the negative gradient of

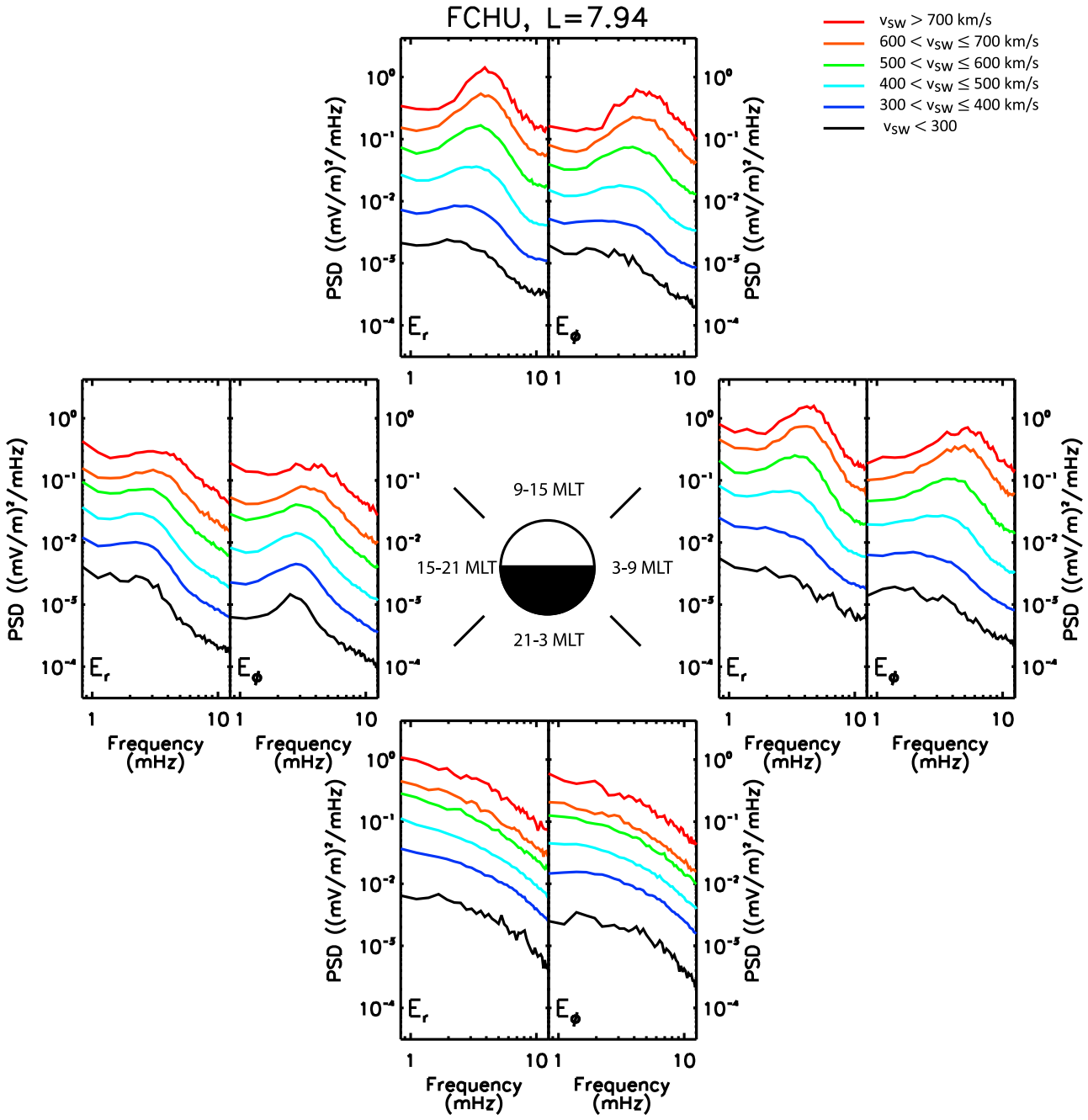

Figure 3. Mapped ULF wave electric field PSD derived from the FCHU magnetometer (L∼7.94), in the same format as Figure 2.

the slope increasing as the frequency increases. Maximum PSD is observed in the dawn sector Er component at GILL, and is largest at high solar wind speeds.

[16] Figures 3–7 show the mapped electric fields derived from ground-based magnetometer data from FCHU (L∼7.94), ISLL (L∼5.40), PINA (L∼4.21), GML (L∼2.98) and YOR (L∼2.55), respectively, all in the same format as Figure 2. All PSDs shown in Figures 3–7 are suppressed relative to their counterparts calculated from the GILL data, and the powers decrease at both higher and lower latitudes. However, all stations observe Gaussian enhancements in the Pc4–5 range at some local times, being clearest at higher solar wind speeds. The Gaussian peaks are also slightly narrower in frequency at FCHU as compared to GILL, the powers reducing to a power law like power spectrum at >10 mHz. The Gaussian peak at ISLL is not as evident at lower solar wind speeds, other than the dusk sector, where the peak is evident under all solar wind speed conditions. At PINA on the nightside, PSD does not decrease very rapidly at higher frequencies, and shows evidence of the start of a secondary peak in the Pc3–4 (15–60 mHz) range (not shown). We leave discussion of any power enhancement outside the Pc4–5 range to a follow-on study. At low solar wind speeds, the powers at the lowest latitudes

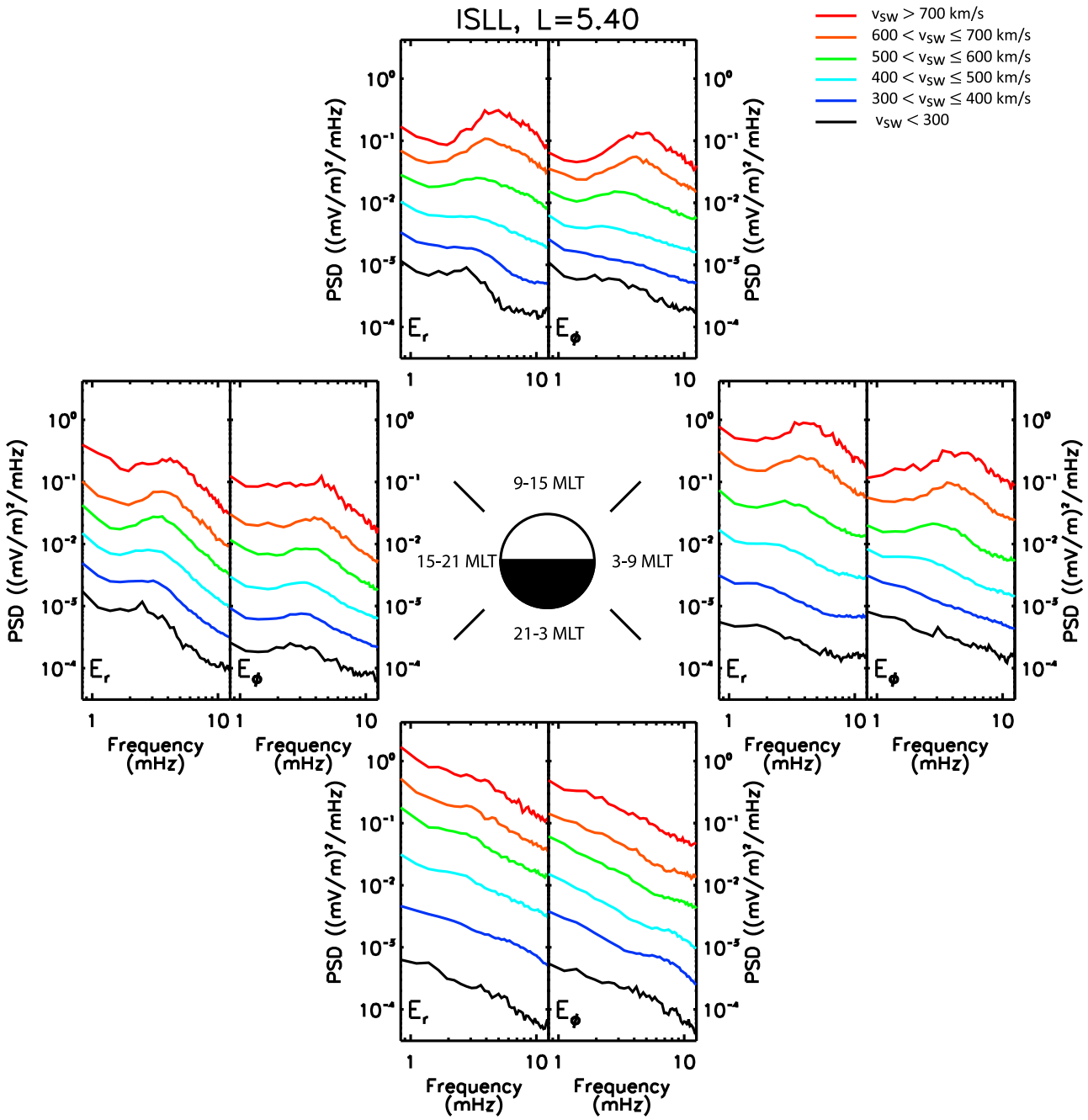

Figure 4. Mapped ULF wave electric field PSD derived from the ISLL magnetometer (L∼5.40), in the same format as Figure 2.

(GML and YOR; Figures 6 and 7) are essentially constant across all frequencies, other than the increase of power at higher frequencies similar to that seen at PINA and which corresponds to a secondary peak in the Pc3–4 band. The median PSDs from YOR (at L∼ 2.55; Figure 7) are remarkably similar to those calculated for GML. One difference between Figures 6 and 7 is that the pronounced power in the secondary Pc3–4 peak is somewhat more pronounced at GML than YOR.

[17] Figure 8 shows a specific example of the L-shell dependence of PSD as a function of frequency for the morning-sector (Figure 8a) H- and D-component averaged median PSDs for the highest solar wind speeds (v_{sw} > 700 km/s), together with (Figure 8b) their equivalent mapped equatorial electric fields Er and Eφ calculated according to *Ozeke et al.* [2009] and as discussed above for the six magnetometers used in this study. Figure 8a demonstrates that in general PSD increases with L-shell from L = 2.5 to 6.5, before decreasing toward higher L-shells at L∼8 [cf. *Engebretson et al.*, 1998; *Mathie and Mann*, 2001] (see also the integrated Pc5 power results obtained by *Pahud et al.* [2009] using this data set). Figure 8b demonstrates that the mapped equatorial electric fields show a significant enhancement of PSD above the

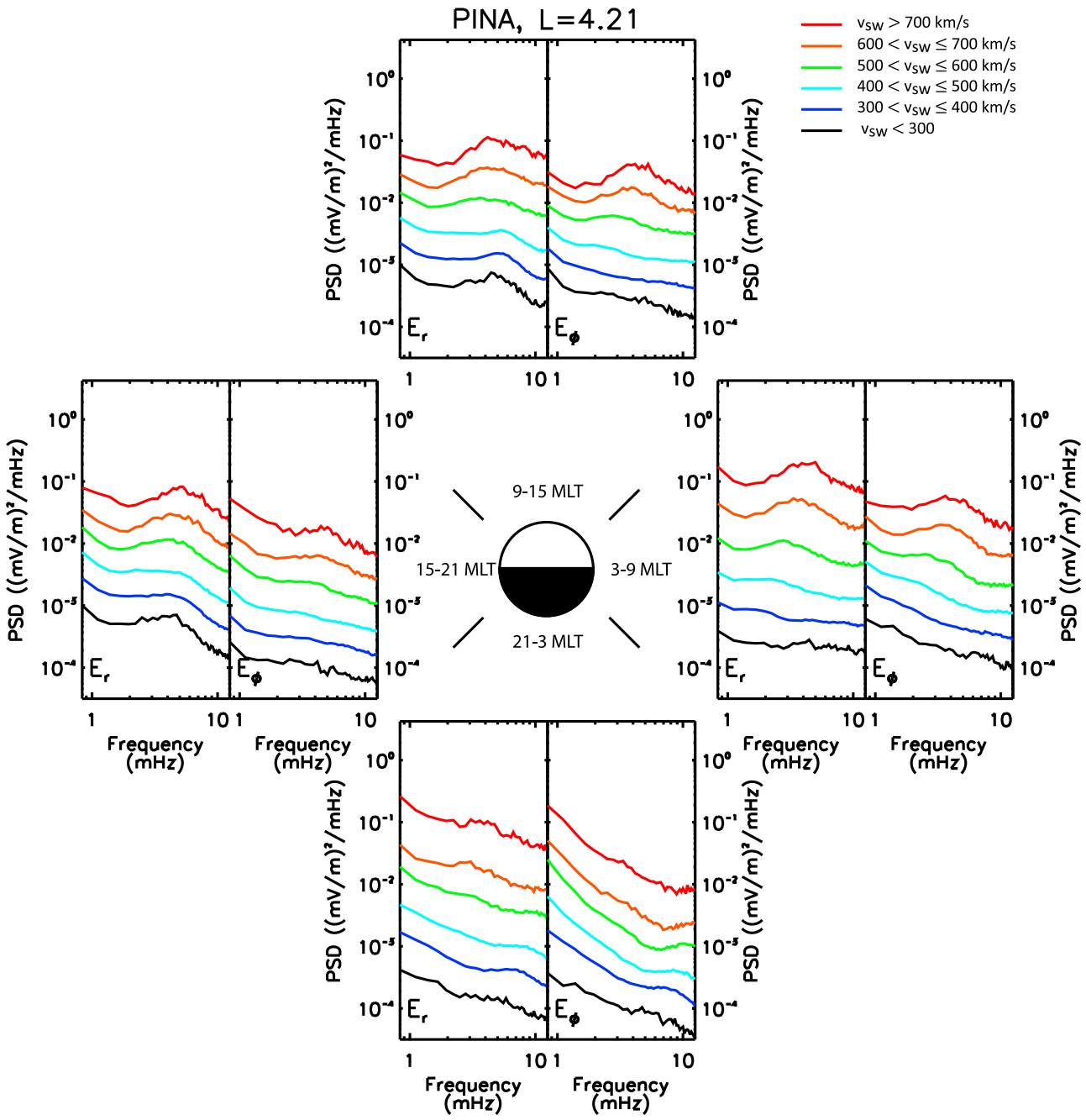

Figure 5. Mapped ULF wave electric field PSD derived from the PINA magnetometer (L∼4.21), in the same format as Figure 2.

background power law due to the Gaussian power peak. Indeed, the mapped electric field PSDs are the highest in the Pc5 ULF wave band in the middle of Gaussian peak, as opposed to lower frequencies. As for the ground, the mapped and inferred equatorial electric fields peak in the auroral zone at the GILL station.

4. Comparison With CRRES Electric Field Spectra [*Brautigam et al.*, 2005]

[18] *Brautigam et al.* [2005] presented electric field observations from a 9 month subset of the ∼14 months of CRRES satellite operation during solar maximum. In their study, *Brautigam et al.* [2005] calculated the median transverse electric field PSD in the Er-Eφ plane as a function of Kp, for different L-shell bins. *Brautigam et al.* [2005] then went on to provide fits for power as a function of L-shell for each frequency and binned these results by Kp. In order to specifically compare the results presented by *Brautigam et al.* [2005] and the results from our ground-space mapping, we compute the median dayside (06–18 MLT) PSDs derived from ground-based magnetometer data as a function of Kp. We then compare the results at three similar L-shells for the three Kp bins that are shown in the *Brautigam et al.*

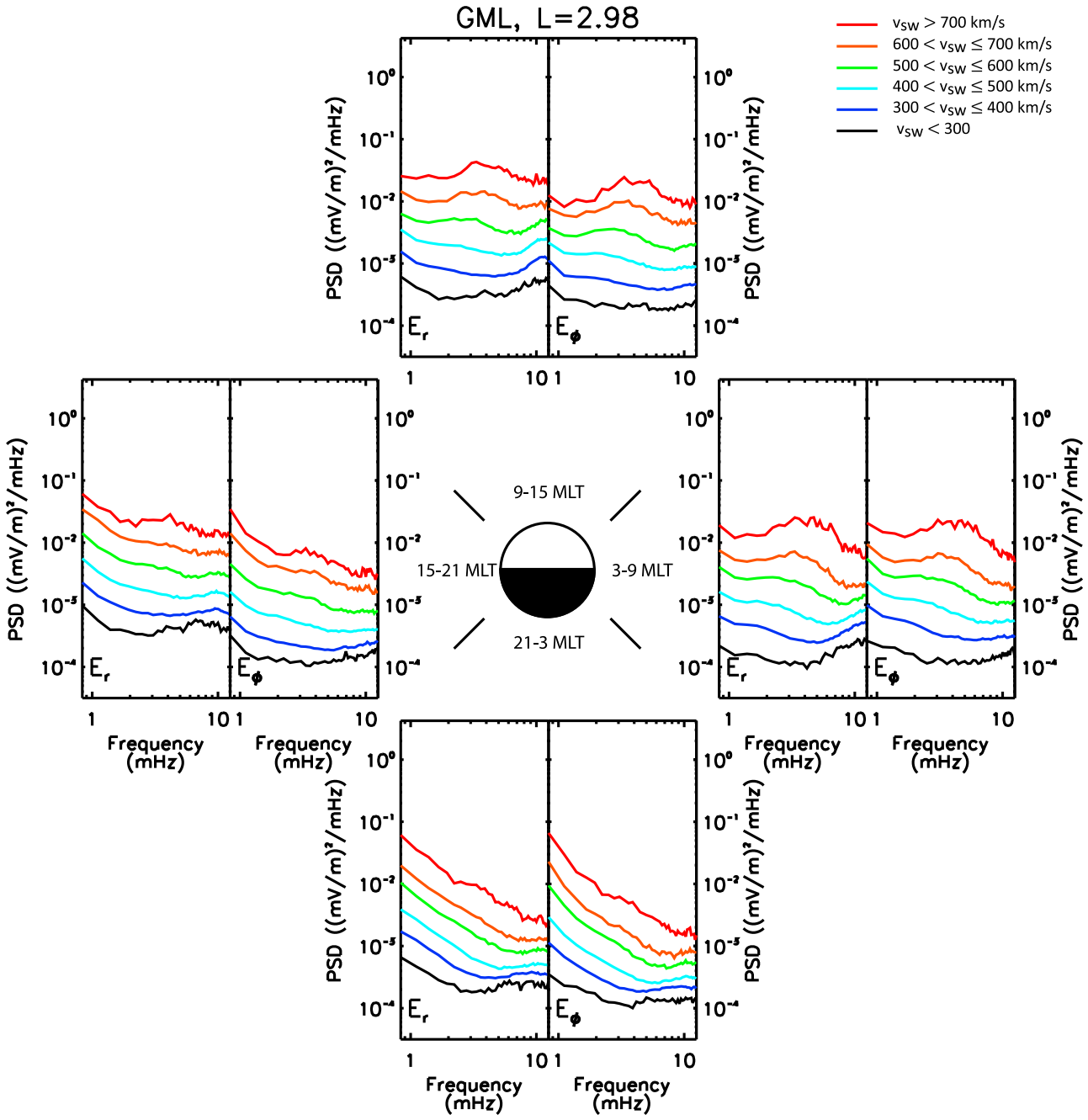

Figure 6. Mapped ULF wave electric field PSD derived from the GML magnetometer (L∼2.98), in the same format as Figure 2.

[2005] paper. Note that the CRRES mission did not traverse all L-shells at all local times before its untimely demise.

[19] Figure 9 shows the results from three stations (PINA, ISLL and GILL) that correspond as closely as possible to the central bin values used by *Brautigam et al.* [2005] in L-shell ranges from L = 3.75–4.25, L = 5.25–5.75 and L = 6.25–6.75. We also note that the *Brautigam et al.* [2005] results represent median L-values throughout their 1 h FFT analysis interval. During such an interval, the authors note that CRRES can move across a large range of L. For example, from L = 2.25 to 5.25 as a worst-case scenario when the satellite was closer to perigee, or from L = 5.25 to 6.75 when the satellite was closer to apogee. This means the in situ powers when binned by the L-shell at the midpoint of the time series used by *Brautigam et al.* [2005] may be artificially enhanced, since CRRES will, in general, spend a longer duration at higher L-shells during any 1 h period. A direct advantage of using ground-based measurements as a proxy for in situ electric fields is the relatively constant location in L-shell of the measurements within a one hour measurement period.

[20] Figure 9 shows that there is excellent comparison at L = 6.5 across all Kp values in both magnitude and shape. In particular, the mapped Eφ electric fields are remarkably

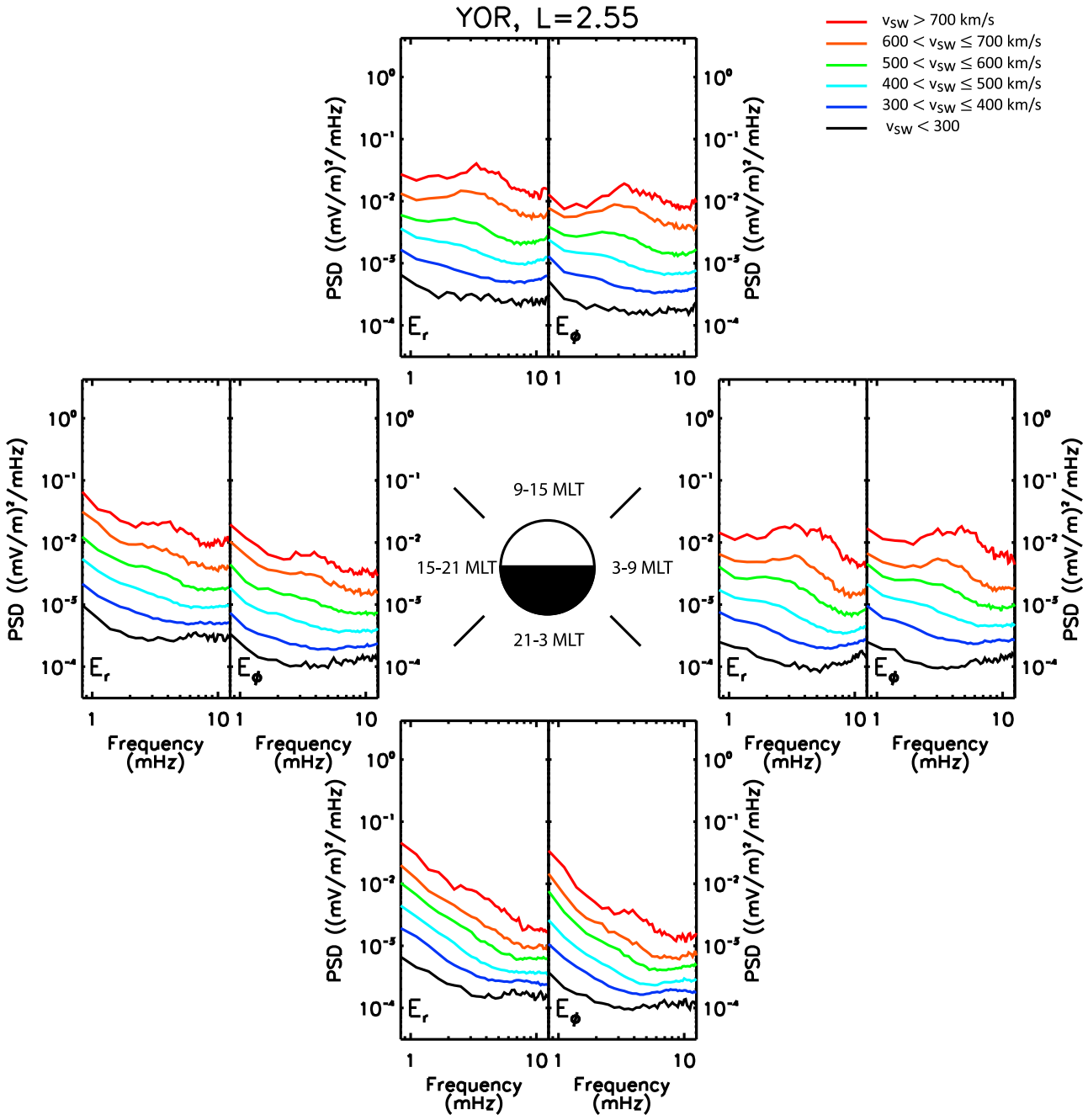

Figure 7. Mapped ULF wave electric field PSD derived from the YOR magnetometer (L∼2.55), in the same format as Figure 2.

consistent with those obtained in situ by *Brautigam et al.* [2005], in particular at moderate Kp. In both spectra, the peak frequencies of the spectral peaks increase with solar wind velocity, and both peaks span primarily the 2–8 mHz range. The low Kp results also have similar absolute power values, but the results presented within this paper for high Kp are larger than those observed by *Brautigam et al.* [2005] by a factor of ∼2 in Eφ, and larger in Er at the highest L at L∼6.5. Figure 9 (middle) shows the equivalent comparison between observations at L = 5.5. Again, there is excellent agreement between our results and those in Brautigam et al.'s study, though there is less low frequency power observed by CRRES than within this study at lower Kp, and the ground-based results again show power larger than that at CRRES at higher Kp. Figure 9 (bottom) shows the same comparison close to L = 4.0. Again, there appears to be smaller powers at lower frequencies in the CRRES results at lower Kp as compared to the results presented in this paper. The peak frequency of the Gaussian peak tends to occur at similar frequencies in both studies for all three L-values and all Kp. Overall, there is excellent agreement in all three L-shell bins, validating the utility of

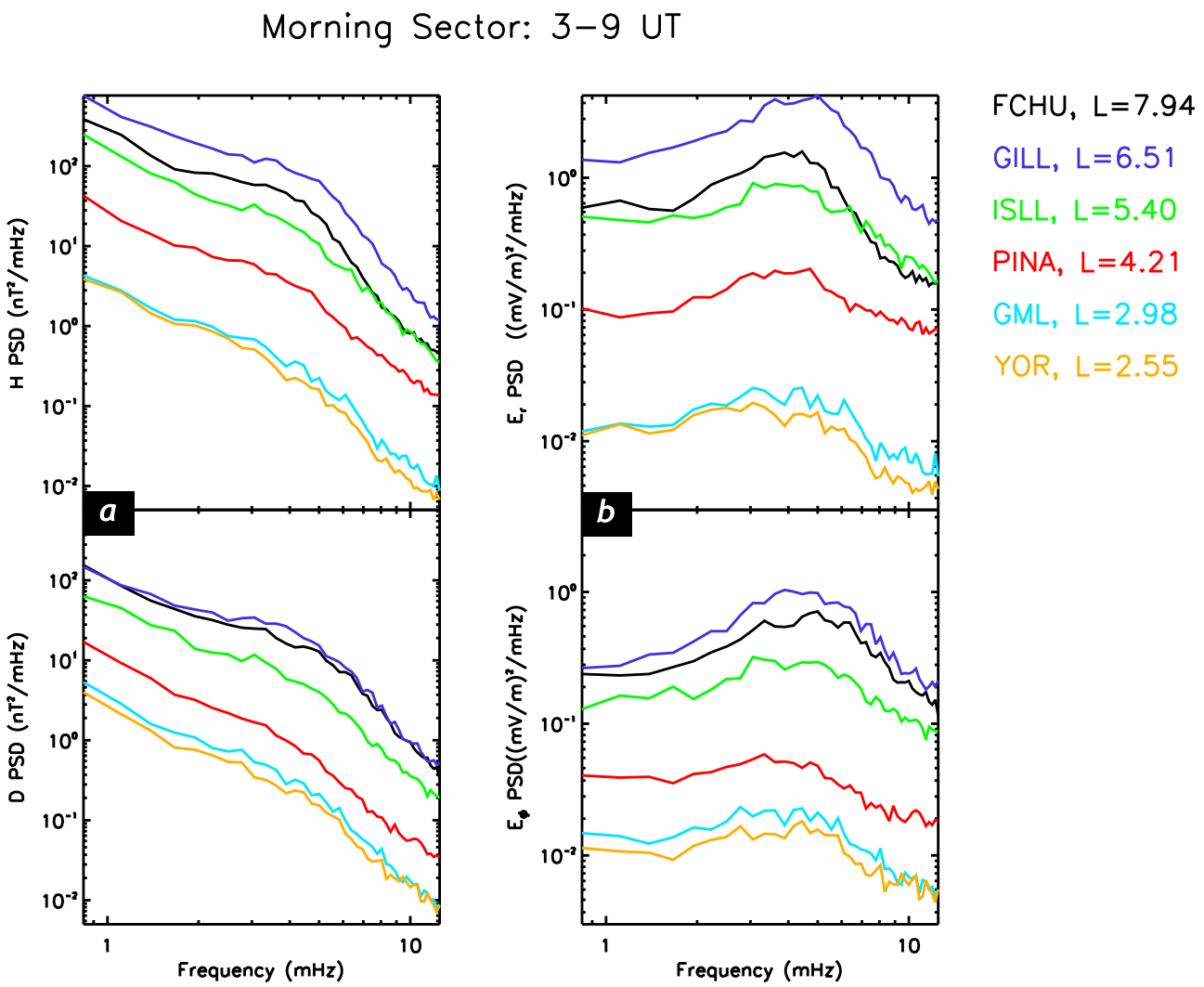

Figure 8. L-shell dependence of (a) ground-based H- and D-component magnetic fields and (b) mapped in situ electric field Er and Eφ electric fields for the highest solar wind speeds (vsw > 700 km/s).

ground-based data for estimating equatorial electric fields in the magnetosphere.

5. Discussion

[21] ULF wave power in the magnetosphere has a well-documented strong dependence on solar wind speed [e.g., *Singer et al.*, 1977; *Rostoker et al.*, 1998; *Engebretson et al.*, 1998; *Mathie and Mann*, 2000, 2001; *O'Brien et al.*, 2001; *Pahud et al.*, 2009]. In a previous statistical study of in situ ULF electric field power [e.g., *Brautigam et al.*, 2005] used Kp to rather than solar wind speed to characterize the waves. In this paper, we use ground-based measurements of magnetic field variations to infer the equatorial magnetospheric electric field PSD (using the *Ozeke et al.* [2009, 2012] model), and study its variation with solar wind velocity, L-shell and MLT. Additionally, and in order to validate our electric fields with the previous study, we also characterized the in situ ULF wave electric field derived from out ground-based magnetometers by Kp.

[22] *Brautigam et al.* [2005] found that there was a strong Kp and L-shell dependence of transverse PSD as a function of frequency, and demonstrated the presence of both a power law and superposed "Gaussian peak" in the PSD spectra as a function of wave frequency. Despite the fact that we derive in situ electric fields from ground-based magnetometer data, we find very similar spectra features. At low L-shells (L < 4), the calculated PSDs had significantly smaller power law exponents than at higher L-shells (L > 4) during more active geomagnetic conditions (Kp > 3). Furthermore, at higher geomagnetic activity (Kp = 6) the background electric field PSDs spectrum is approximately constant across all frequencies, and the power in the Gaussian peaks dominates. We find an excellent qualitative and quantitative agreement between the electric fields derived from ground-based magnetometer data and those derived by *Brautigam et al.* [2005] (Figure 8). The dawn local time sector (~0300–1200 MLT) did not form a large part of the statistics compiled by *Brautigam et al.* [2005], which is where the occurrence and amplitude of Pc5 wave power reaches a maximum [e.g., *Engebretson et al.*, 1998; *Posch et al.*, 2003; *Pahud et al.*, 2009]. By using the ground-based magnetic field measurements to infer equatorial

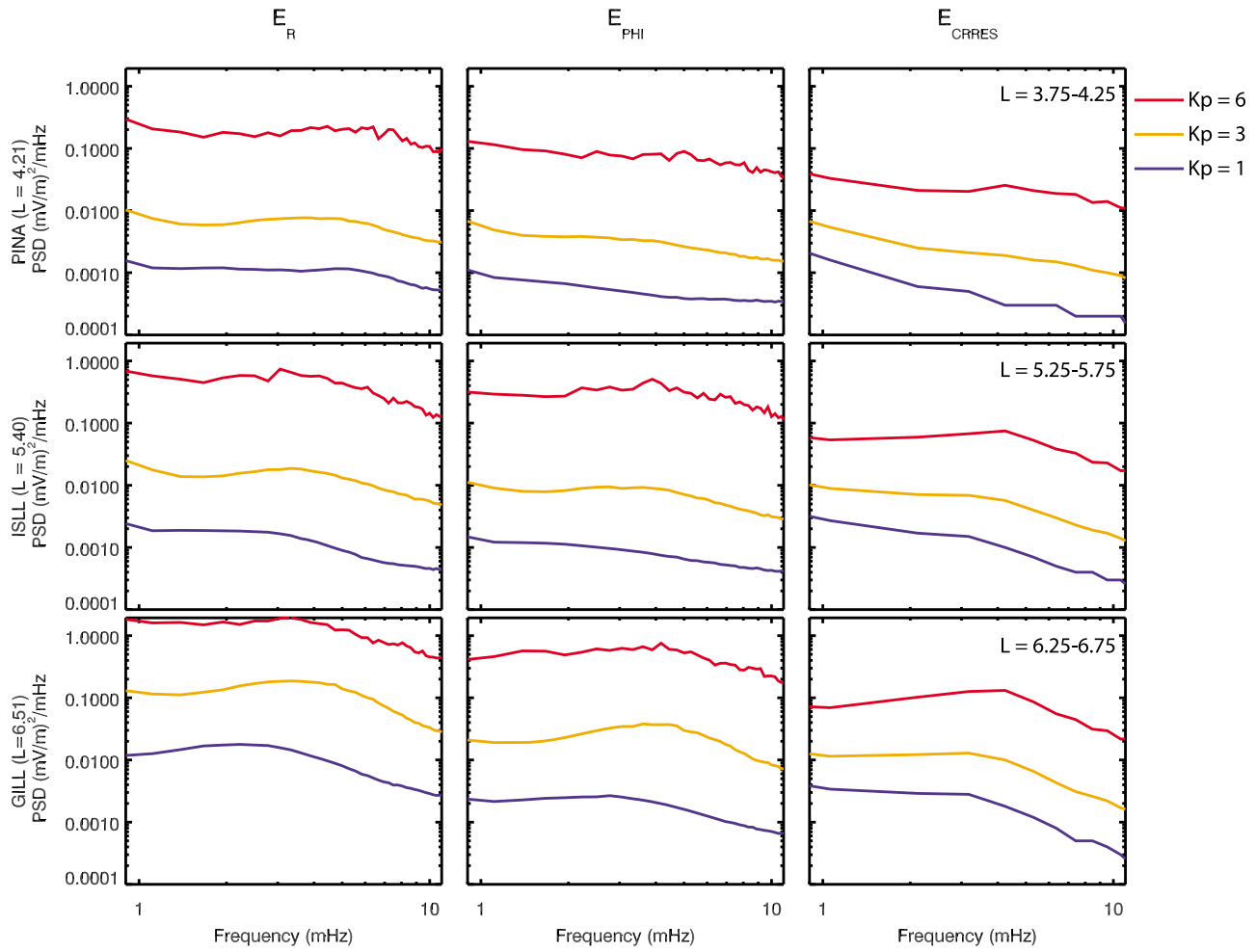

Figure 9. Comparison of the mapped electric fields and fits to the transverse electric field observed by CRRES and tabled by *Brautigam et al.* [2005]. Shown are the comparison of the (left) Er and (middle) Eφ median PSDs from our mapped ground-based results as a function of Kp, and (right) *Brautigam et al.* [2005] fits to in situ transverse electric field power for the same Kp values. Also shown are comparisons between the results for different Kp bins at (top) L$\sim$4.0, (middle) L$\sim$5.5, and (bottom) L$\sim$6.5.

electric field wave amplitudes, we can extend previous studies of ULF electric field wave power to extract and characterize the strong MLT dependence. Based upon the successful ground-based estimation of the electric fields in the magnetosphere, we assert that the wave statistics reported in this paper represent an excellent basis for describing the expected ULF wave power in the magnetosphere based on the characteristics of driving and incident solar wind speed or prevalent Kp.

[23] Previous studies have shown that the Pc5 ULF wave power in the integrated 1–2 to 10 mHz power range in the morning side increases significantly when the solar wind speed is in excess of 500 km/s [e.g., *Engebretson et al.*, 1998; *Mathie and Mann*, 2001; *Pahud et al.*, 2009]. *Mathie and Mann* [2001] presented the statistics of dawn sector Pc5 PSD as a function of solar wind speed for ground magnetometer stations between L = 3.75–6.79. In their paper, these authors found a monotonic increase of solar wind power as a function of L-shell in this L-shell range. In this study, we extend the L-shell range to both lower and higher values. We find that the ULF wave powers continue to decrease toward lower L-shells, but at higher L-shells (L$\sim$8), the ULF powers also begins to decrease. The results of this study therefore extend the findings of previous integrated Pc5 power studies such as *Engebretson et al.* [1998] and *Mathie and Mann* [2001], providing additional local time information and, more importantly, new spectral information about the ULF wave power which has not previously been reported. Significant discrete peaks in the power spectra occur at noon and dawn, with the largest overall ULF wave power being seen at midnight. Midnight, however, is usually characterized by a simple single index power law distribution.

[24] In general, the morning, noon and dusk ULF electric field PSD spectra can be considered to be comprised of two parts: a localized Gaussian centered at a specific frequency superimposed on a single index power law. In general, the power law index, p, characterizing power P α f^{-p}, increases with L-shell (compare Figures 2 through 7). The localized Gaussian peaks are the largest and most distinct in the

morning sector, followed by the noon sector and finally the dusk sector. A number of studies have discussed the asymmetry of ground-based dawn and dusk side Pc5 wave activity, and these studies show similar results as described above and within this paper [e.g., *Gupta*, 1975; *Ziesolleck and McDiarmid*, 1994; *Chisham and Orr*, 1997; *Glassmeier and Stellmacher*, 2000; *Baker et al.*, 2003]. Potential explanations of the clear dawn-dusk asymmetry range from the orientation of the Parker spiral angle [e.g., *Gupta*, 1975], a change in polarization across noon [e.g., *Olson and Rostoker*, 1978], or ionospheric screening effects [e.g., *Hughes and Southwood*, 1976]. Generally, azimuthal wave number effects are proposed to explain any asymmetry of dawn-dusk ULF wave activity, specifically that higher-m ULF waves may be preferentially generated in the post-noon sector [e.g., *Yumoto et al.*, 1983]. However, radial gradients in plasma density may lead to local time variations in the latitudinal width of the resonance, which may be of equal importance [*Glassmeier and Stellmacher*, 2000]. These effects are not necessarily mutually exclusive, and therefore additively contribute to the clear dawn-dusk asymmetry observed by these authors and also demonstrated within this paper. We assert that the Gaussian peaks detailed within this paper are most likely due to FLR-driven energy accumulation in the L = 4–7 range. The lack of a Gaussian enhancement on the nightside may be a consequence of low ionospheric Pedersen conductivity, which does not support field line resonances in locations where the Alfvén and Pedersen conductances are similar [*Ellis and Southwood*, 1983; *Ozeke and Mann*, 2004]. Consequently, the FLRs that we propose are the cause of the peaks in the PSD are not observed on the nightside and so the PSD can be generally characterized by a power law both on the ground and in space.

[25] That the nightside ULF PSD can be characterized by a power law is well known, both for in situ and ground-based measurements [e.g., *Arthur et al.*, 1978; *Francia et al.*, 1995; *Weatherwax et al.*, 2000; *Murphy et al.*, 2011]. However, there are few studies detailing the power law plus Gaussian enhancement/peak nature of geomagnetic activity at other local times [e.g., *Bloom and Singer*, 1995; *Brautigam et al.*, 2005; *Murphy et al.*, 2011]. *Bloom and Singer* [1995] presented low-mid latitude observations of ground spectral powers as a function of local time in specific Pc4–5 ULF wave frequency ranges. *Bloom and Singer* [1995] found that there was evidence of enhanced spectral power near 55° latitude in the 2–6 mHz frequency range across the dayside region, which is consistent with the results we obtain at those latitudes (see Figure 1 and Figure S1 in the auxiliary material).[1]

[26] Figure 8 shows that the central frequency of the Gaussian enhancement has some tendency to increase with decreasing L-shell, which is consistent with the excitation of standing Alfvén waves in the magnetosphere. However, the peak is observed at most solar wind speeds, and across all dayside local times, raising the question as to how this statistical behavior is consistent with previous case studies of a dominant and typically much narrower discrete Pc5 spectral peak on any given day in the morning sector. *Baker et al.* [2003] presented statistical results of monochromatic FLR events from the CANOPUS/CARISMA ground-based "Churchill Line" magnetometers strictly in the Pc5 (1.67–6.67 mHz) frequency band and identified FLRs by visual inspection, finding that there was a strong peak in FLR activity in the morning sector, a secondary peak in activity around dusk, and no occurrence peak in the noon sector. The peak in Pc5 event occurrence in the morning sector and a secondary peak in the afternoon sector are consistent with the results obtained by *Baker et al.* [2003], and with our results showing a FLR-like discrete spectral peak in the median spectra at both dawn and dusk local times. In this study we find evidence of a Gaussian enhancement in the median spectra observed in the noon sector which, if due to a superposition of events with narrower spectral FLR peaks for different days and conditions, might have been expected to be also clearly seen in the ground-based event statistics of *Baker et al.* [2003]. Note, however, that *Baker et al.* [2003] did observe events around local noon, just a larger occurrence of FLRs at dawn and at dusk. *Plaschke et al.* [2008] demonstrate that the most likely occurrence location on the ground for Pc5 FLRs is in the 65–70°CGM latitude range, i.e., locations corresponding to GILL-FCHU used in this study. Furthermore, *Plaschke et al.* [2008] showed clear evidence of significant occurrence of FLRs in the noon sector, detected with the wave telescope method. Hence, the *Plaschke et al.* [2008] results are in good agreement with this study.

[27] Perhaps the strongest evidence linking this Gaussian enhancement in the PSD to FLR activity has been shown recently by *Takahashi et al.* [2010] and *Murphy et al.* [2011]. *Takahashi et al.* [2010] used over one solar cycle of GOES geosynchronous magnetic field data to show that the frequency of the third harmonic field line resonance was anti-correlated with F10.7 solar radio flux. These authors interpreted this result as evidence of a solar cycle dependence in the equatorial mass density, which in turn affects the field line resonance eigenperiods of the geomagnetic field lines. Following on from *Takahashi et al.* [2010], *Murphy et al.* [2011] analyzed a sub-section of the database described in section 2 to investigate whether the locations in frequency of the Gaussian enhancements observed on the ground were also dependent on solar cycle. *Murphy et al.* [2011] demonstrated clearly that, although the exponent of the ULF wave power law spectrum did not change significantly through the solar cycle, the central frequency of the Gaussian enhancement observed in ground magnetometer data was indeed inversely proportional to both F10.7 and L shell, i.e., the Gaussian peak frequency decreased with increasing F10.7 fluxes and increasing L shell. Together with the results shown by *Takahashi et al.* [2010], this presents strong evidence that the source of the Gaussian enhancements superimposed on the PSD power law seen in the median power spectra can be explained by an accumulation of energy via field line resonance. Finally, it must be noted that if these spectral peaks do indeed represent FLR activity, our results provide clear statistical evidence that, at least when it is described by median spectra, the magnetosphere does not generally exhibit specific and repeatable

[1]Auxiliary material is available in the HTML. doi:10.1029/2011JA017335.

"magic frequencies" [*Samson et al.*, 1992]; rather, the magic frequencies form part of a continuum of geomagnetic activity that is controlled by the density distribution and field line topology within the magnetosphere. Note, however, that this does not preclude the occurrence of individual events with clear and narrow-band discrete FLR signatures, nor specifically in terms of event occurrence rate that some frequencies within the continuum may occur more often than others.

[28] It is interesting to note that the FLR frequencies reported by *Samson et al.* [1992; see also, e.g., *Ruohoniemi et al.*, 1991; *Walker et al.*, 1992; *Ziesolleck and McDiarmid*, 1994] were centered around a series of discrete values around 1.3, 1.9, 2.6–2.7, 3.2–3.4 mHz etc. Subsequent work, such as *Mathie et al.* [1999], demonstrated that when narrow-band FLR events were selected from ground-based magnetometer time series there were peaks in FLR occurrence in bands that contain the "Samson" frequencies. However, these occurrence peaks at the "Samson" frequencies given by *Samson et al.* [1992] were not unique between 1 and 4 mHz. *Mathie et al.* [1999] therefore suggested that this distribution may be explained by variability in the eigenfrequencies of the waveguide from day to day and under differing geomagnetic activity, magnetic field, and mass density distributions inside the waveguide [see *Mathie et al.*, 1999, Figure 3].

[29] Assuming that events at the "Samson" frequencies are both preferred and of sufficiently high amplitude, it might be expected that waves at these narrow-band frequencies should appear in the ground-based median PSD power spectra results presented in this paper. Such amplitude peaks were found by *Villante et al.* [2001] in the post-noon sector of a 2 year statistical analysis of low-L (L = 1.6) ground magnetometer data, being most obvious at high solar wind pressures, during conditions which presumably significantly compress the magnetospheric cavity. Power peaks were also found by Villante et al. using a statistical ULF wave power analysis during the interval of the *Mathie et al.* [1999] event analysis, but these power peaks were not clearly statistically significant. More recently, *Plaschke et al.* [2009] used seven months of THEMIS magnetic field data [e.g., *Auster et al.*, 2009]. In order to characterize magnetopause motion in a period of low solar activity, these authors finding clear occurrence peaks in the magnetopause oscillation frequencies at Samson frequencies. Although the lower-frequency part of our median power spectra show some small variations superposed on top of a power law plus Gaussian distribution, they do not show fine structure with peaks at the "Samson frequencies." The question is why?

[30] First, a median power spectra derived from a superposition of events, even a superposition of a series of "narrow band" FLR events, will demonstrate less clear peaks in frequency than a histogram of the occurrence distribution of the frequency of the peak power value alone. Second, narrow band FLR events only represent one element of the overall Pc4–5 power spectra in the 1–10 mHz band once the median values of power at each bin for the entire distribution of events from all days is calculated. Certainly there can also be significant power contained in the Pc5 band in events whose frequencies are not narrow band, such as from broadband fast mode wave sources which drive standing Alfvén waves either locally or over a broad range of latitudes [cf. *Hasegawa et al.*, 1983]. Further contributions in the ground spectra may arise from changes in ionospheric currents from, for example, changes in ionspheric conductivity, which may not have any clear magnetospheric ULF wave counterpart. However, even with these provisos one might still expect a signature of the "Samson" frequency fine structure to remain if they represent a statistically preferred set of frequencies which accumulate power.

[31] Probably the principal reason for the discrepancy is variation in FLR frequencies. *Takahashi et al.* [2010] showed that the FLR eigenfrequencies of standing Alfvén waves seen at geosynchronous orbit can change by a factor of ~2 over a solar cycle, due to solar cycle dependence of the ambient mass density (independently verified by *Murphy et al.* [2011] using the ground-based data set presented here). This will change the FLR frequency on the ground at a station at a given invariant latitude, almost certainly contributing to the smoothing of the median power spectra seen on the ground when data from an entire solar cycle are combined. If the "Samson" frequencies are signatures of the eigenmodes of the magnetospheric waveguide, the frequencies of the waveguide modes which are determined by a phase integral across the non-uniform waveguide may also change not only from day to day with geomagnetic activity (as *Mathie et al.* [1999] suggested), but also on average across the solar cycle as a result of the density changes inferred by *Takahashi et al.* [2010]. Such effects would smooth the median spectra, perhaps removing evidence of fine structure of power accumulation at the "Samson" frequencies, leaving instead a broader spectral peak from ~1–4 mHz in median spectra like that reported here where the FLR power accumulates. However, since *Samson et al.* [1992], *Mathie et al.* [1999], and *Villante et al.* [2001] all showed some evidence of either narrow-band spectral peaks in occurrence or power during periods of strong solar wind driving, either during solar maximum, during high solar wind speed streams during the declining phase, or during intervals of high solar wind dynamic pressure, but the *Plaschke et al.* [2009] study showed clear evidence of occurrence peaks during low solar wind driving, it is clear that more work is required to study the dependence of median ULF wave power spectra fine structure on solar cycle phase.

[32] The amplitudes of the H- and D- component PSDs are approximately equal at lower L-shells (e.g., GML and YOR, Figures 5 and 6, respectively), but at mid-high L-shells and in particular for higher solar wind speeds, the H-component PSDs can be over two times larger than the D-component PSDs. This additional PSD implies additional energy accumulation in the H-component wave field as compared to the D-component, perhaps another strong indication that the Gaussian enhancement is related to toroidal-mode FLRs [e.g., *Takahashi et al.*, 2010; *Murphy et al.*, 2011]. In general the H- component power typically dominates the D-component power, which under an Alfvénic approximation and 90° rotation through the ionosphere, translates to a larger Er component than $E\varphi$ in the equatorial magnetosphere. Since both Er and $E\varphi$ are strongly peaked on the dayside, the contribution of the Gaussian ULF wave spectral enhancement must be taken into account when defining

the PSD in the Pc4–5 ULF wave band for radiation belt modeling purposes. In an azimuthally symmetric magnetic field all of the electron energization is due to the Eφ component, however in non-azimuthally symmetric magnetic fields such as a compressed dipole then the Er component can also provide electron energization [e.g., *Elkington et al.*, 1999, 2003]. Hence both the Er and Eφ results presented in this paper represent important parameterization for specifying the role of Pc4–5 waves in radiation belt dynamics under the action of radial diffusion.

6. Conclusions

[33] In this paper, we use ~15 years of data from the CANOPUS/CARISMA and SAMNET magnetometer arrays in order to statistically characterize the ground-based H- and D-component magnetic Pc5 ULF wave spectrum as a function of solar wind speed, L-shell and MLT. We find that, in general, ULF wave activity can be described by a power law like power spectrum with a superposed localized Gaussian enhancement centered at a specific frequency superimposed on this power law at all local times other than midnight. The midnight sector PSD is best described as a simple power law.

[34] We use a guided Alfvén wave approximation detailed by *Ozeke et al.* [2009, 2012] in order to map these ground-based magnetic fields into azimuthal and radial equatorial magnetospheric electric fields. We find that the in situ electric field power laws have shallower exponents in space, and that in general the Gaussian enhancements become much more pronounced, revealing that Field Line Resonances provide energetically significant ULF wave power that should not be ignored when ascribing ULF wave fields for inclusion into radiation belt radial diffusion models. We find excellent agreement between our ground-based estimates of electric field and the transverse electric field ULF wave powers observed in situ with CRRES by *Brautigam et al.* [2005], over the L-shell ranges that were studied within this paper. This demonstrates the utility of using ground-based magnetometer data in order to prescribe equatorial electric fields as a function of solar wind driving conditions for input into radiation belt radial diffusion models. The accurate determination of both electric and magnetic diffusion coefficients is critical for understand the influence that ULF waves have on the dynamics and energization of electrons in the outer radiation belt region, and the results presented here provide the basis of the development of new physics-based empirical electric diffusion coefficients based directly on ULF wave observations.

[35] **Acknowledgments.** I.J.R., L.G.O., and D.K.M. are funded by the Canadian Space Agency. I.R.M. is supported by a Canadian NSERC Discovery Grant. K.R.M. is funded by Alberta Innovates and an NSERC Canadian Graduate Scholarship. CARISMA is operated by the University of Alberta and funded by the Canadian Space Agency. The Sub-Auroral Magnetometer Network data (SAMNET) is operated by the Department of Communications Systems at Lancaster University (UK) and is funded by the Science and Technology Facilities Council (STFC). This work was supported in part from NASA grants NNX08AM36G and NNX10AL02G. The authors are indebted to D. Wallis for the management and operation of the CANOPUS magnetometer network for the majority of the period studied within this manuscript, and D. M. Pahud for the initial compilation and analysis of CARISMA data within this database.

[36] Robert Lysak thanks the reviewers for their assistance in evaluating this paper.

References

Arthur, C., R. Mcpherron, L. Lanzerotti, and D. Webb (1978), Geomagnetic-field fluctuations at synchronous orbit: 1. Power spectra, *J. Geophys. Res.*, *83*, 3859–3865, doi:10.1029/JA083iA08p03859.

Auster, H. U., et al. (2009), The THEMIS fluxgate magnetometer, *Space Sci. Rev.*, *141*, 235–264, doi:10.1007/s11214-008-9365-9.

Baker, D. N. (2002), How to cope with space weather, *Science*, *297*(5586), 1486–1487, doi:10.1126/science.1074956.

Baker, D. N., T. Pulkkinen, X. Li, S. Kanekal, J. Blake, R. Selesnick, M. Henderson, G. Reeves, H. Spence, and G. Rostoker (1998a), Coronal mass ejections, magnetic clouds, and relativistic magnetospheric electron events: ISTP, *J. Geophys. Res.*, *103*, 17,279–17,291, doi:10.1029/97JA03329.

Baker, D., et al. (1998b), A strong CME-related magnetic cloud interaction with the Earth's magnetosphere: ISTP observations of rapid relativistic electron acceleration on May 15, 1997, *Geophys. Res. Lett.*, *25*, 2975–2978, doi:10.1029/98GL01134.

Baker, G., E. Donovan, and B. Jackel (2003), A comprehensive survey of auroral latitude Pc5 pulsation characteristics, *J. Geophys. Res.*, *108*(A10), 1384, doi:10.1029/2002JA009801.

Bloom, R., and H. Singer (1995), Diurnal trends in geomagnetic noise power in the Pc-2 through Pc-5 bands at low geomagnetic latitudes, *J. Geophys. Res.*, *100*, 14,943–14,953, doi:10.1029/95JA01332.

Brautigam, D., and J. Albert (2000), Radial diffusion analysis of outer radiation belt electrons during the October 9, 1990, magnetic storm, *J. Geophys. Res.*, *105*, 291–309, doi:10.1029/1999JA900344.

Brautigam, D., G. Ginet, J. Albert, J. Wygant, D. Rowland, A. Ling, and J. Bass (2005), CRRES electric field power spectra and radial diffusion coefficients, *J. Geophys. Res.*, *110*, A02214, doi:10.1029/2004JA010612.

Brizard, A., and A. Chan (2001), Relativistic bounce-averaged quasilinear diffusion equation for low-frequency electromagnetic fluctuations, *Phys. Plasmas*, *8*, 4762–4771, doi:10.1063/1.1408623.

Brizard, A., and A. Chan (2004), Relativistic quasilinear diffusion in axisymmetric magnetic geometry for arbitrary-frequency electromagnetic fluctuations, *Phys. Plasmas*, *11*, 4220–4229, doi:10.1063/1.1773554.

Chisham, G., and D. Orr (1997), A statistical study of the local time asymmetry of Pc5 ULF wave characteristics observed at midlatitudes by SAMNET, *J. Geophys. Res.*, *102*, 24,339, doi:10.1029/97JA01801.

Degeling, A. W., R. Rankin, K. Kabin, R. Marchand, and I. R. Mann (2007), The effect of ULF compressional modes and field line resonances on relativistic electron dynamics, *Planet. Space Sci.*, *55*, 731–742, doi:10.1016/j.pss.2006.04.039.

Degeling, A. W., R. Rankin, K. Kabin, I. J. Rae, and F. R. Fenrich (2010), Modeling ULF waves in a compressed dipole magnetic field, *J. Geophys. Res.*, *115*, A10212, doi:10.1029/2010JA015410.

Dungey, J. W. (1955), Electrodynamics of the outer atmosphere, in *Proceedings of the Ionosphere Conference*, p. 255, Phys. Soc. of London, London.

Elkington, S., M. Hudson, and A. Chan (1999), Acceleration of relativistic electrons via drift-resonant interaction with toroidal-mode Pc5 ULF oscillations, *Geophys. Res. Lett.*, *26*, 3273–3276, doi:10.1029/1999GL003659.

Elkington, S., M. Hudson, and A. Chan (2003), Resonant acceleration and diffusion of outer zone electrons in an asymmetric geomagnetic field, *J. Geophys. Res.*, *108*(A3), 1116, doi:10.1029/2001JA009202.

Ellis, P., and D. Southwood (1983), Reflection of Alfvén waves by non-uniform ionospheres, *Planet. Space Sci.*, *31*, 107–117, doi:10.1016/0032-0633(83)90035-1.

Engebretson, M., K. Glassmeier, M. Stellmacher, W. Hughes, and H. Luhr (1998), The dependence of high-latitude Pc5 wave power on solar wind velocity and on the phase of high-speed solar wind streams, *J. Geophys. Res.*, *103*, 26,271–26,283, doi:10.1029/97JA03143.

Fälthammar, C. G. (1965), Effects of time-dependent electric fields on geomagnetically trapped radiation, *J. Geophys. Res.*, *70*, 2503–2516, doi:10.1029/JZ070i011p02503.

Francia, P., U. Villante, and A. Meloni (1995), An analysis of geomagnetic-field variations (3-Min 2-H) at a low-latitude observatory (L = 1.6), *Ann. Geophys.*, *13*, 522–531.

Friedel, R., G. Reeves, and T. Obara (2002), Relativistic electron dynamics in the inner magnetosphere—A review, *J. Atmos. Sol. Terr. Phys.*, *64*, 265–282, doi:10.1016/S1364-6826(01)00088-8.

Glassmeier, K.-H., and M. Stellmacher (2000), Concerning the local time asymmetry of Pc5 wave power at the ground and field line resonance widths, *J. Geophys. Res.*, *105*, 18,847–18,855, doi:10.1029/2000JA900037.

Gupta, J. C. (1975), Some characteristics of large amplitude Pc 5 pulsations, *Aust. J. Phys.*, *29*, 67.

Hasegawa, A., K. H. Tsui, and A. S. Assis (1983), A theory of long period magnetic pulsations: 3. Local field line oscillations, *Geophys. Res. Lett.*, *10*(8), 765–767, doi:10.1029/GL010i008p00765.

Hasegawa, H., M. Fujimoto, T. Phan, H. Reme, A. Balogh, M. Dunlop, C. Hashimoto, and R. Tandokoro (2004), Transport of solar wind into Earth's magnetosphere through rolled-up Kelvin-Helmholtz vortices RID A-1192–2007, *Nature*, *430*, 755–758, doi:10.1038/nature02799.

Huang, C., H. E. Spence, H. J. Singer, and W. J. Hughes (2010), Modeling radiation belt radial diffusion in ULF wave fields: 1. Quantifying ULF wave power at geosynchronous orbit in observations and in global MHD model, *J. Geophys. Res.*, *115*, A06215, doi:10.1029/2009JA014917.

Hudson, M. K., S. R. Elkington, J. G. Lyon, M. Wiltberger, and M. Lessard (2001), Radiation belt electron acceleration by ULF wave drift resonance: Simulation of 1997 and 1998 storms, *Space Weather*, *125*, 289–296, doi:10.1029/GM125p0289.

Hughes, W. J., and D. J. Southwood (1976), The screening of micropulsation signals by the atmosphere and the ionosphere, *J. Geophys. Res.*, *81*, 3234–3240, doi:10.1029/JA081i019p03234.

Jacobs, J., S. Matsushita, Y. Kato, and V. Troitskaya (1964), Classification of geomagnetic micropulsations, *J. Geophys. Res.*, *69*, 180–181, doi:10.1029/JZ069i001p00180.

Lee, E. A., I. R. Mann, T. M. Loto'aniu, and Z. C. Dent (2007), Global Pc5 pulsations observed at unusually low L during the great magnetic storm of 24 March 1991, *J. Geophys. Res.*, *112*, A05208, doi:10.1029/2006JA011872.

Mann, I., A. Wright, K. Mills, and V. Nakariakov (1999), Excitation of magnetospheric waveguide modes by magnetosheath flows, *J. Geophys. Res.*, *104*, 333–353, doi:10.1029/1998JA900026.

Mann, I., et al. (2002), Coordinated ground-based and Cluster observations of large amplitude global magnetospheric oscillations during a fast solar wind speed interval RID E-7533–2011, *Ann. Geophys.*, *20*, 405–426, doi:10.5194/angeo-20-405-2002.

Mann, I. R., et al. (2008), The upgraded CARISMA magnetometer array in the THEMIS era, *Space Sci. Rev.*, *141*, 413–451, doi:10.1007/s11214-008-9457-6.

Mathie, R., and I. Mann (2000), Observations of Pc5 field line resonance azimuthal phase speeds: A diagnostic of their excitation mechanism, *J. Geophys. Res.*, *105*, 10,713–10,728, doi:10.1029/1999JA000174.

Mathie, R., and I. Mann (2001), On the solar wind control of Pc5 ULF pulsation power at mid-latitudes: Implications for MeV electron acceleration in the outer radiation belt, *J. Geophys. Res.*, *106*, 29,783–29,796, doi:10.1029/2001JA000002.

Mathie, R., I. Mann, F. Menk, and D. Orr (1999), Pc5 ULF pulsations associated with waveguide modes observed with the IMAGE magnetometer array, *J. Geophys. Res.*, *104*, 7025–7036, doi:10.1029/1998JA900150.

Mills, K., A. Wright, and I. Mann (1999), Kelvin-Helmholtz driven modes of the magnetosphere, *Phys. Plasmas*, *6*, 4070–4087, doi:10.1063/1.873669.

Murphy, K. R., I. R. Mann, I. J. Rae, and D. K. Milling (2011), Dependence of ground-based Pc5 ULF wave power on F10.7 solar radio flux and solar cycle phase, *J. Atmos. Sol. Terr. Phys.*, *73*, 1500–1510, doi:10.1016/j.jastp.2011.02.018.

O'Brien, T., R. McPherron, D. Sornette, G. Reeves, R. Friedel, and H. Singer (2001), Which magnetic storms produce relativistic electrons at geosynchronous orbit?, *J. Geophys. Res.*, *106*, 15,533–15,544, doi:10.1029/2001JA000052.

Olson, J. V., and G. Rostoker (1978), Longitudinal phase variations of Pc 4–5 micropulsations, *J. Geophys. Res.*, *83*, 2481–2488, doi:10.1029/JA083iA06p02481.

Ozeke, L., and I. Mann (2004), Modeling the properties of guided poloidal Alfvén waves with finite asymmetric ionospheric conductivities in a dipole field, *J. Geophys. Res.*, *109*, A05205, doi:10.1029/2003JA010151.

Ozeke, L. G., I. R. Mann, and I. J. Rae (2009), Mapping guided Alfvén wave magnetic field amplitudes observed on the ground to equatorial electric field amplitudes in space, *J. Geophys. Res.*, *114*, A01214, doi:10.1029/2008JA013041.

Ozeke, L. G., I. R. Mann, K. R. Murphy, I. J. Rae, D. K. Milling, S. R. Elkington, A. A. Chan, and H. J. Singer (2012), ULF wave derived radiation belt radial diffusion coefficients, *J. Geophys. Res.*, *117*, A04222, doi:10.1029/2011JA017463.

Pahud, D. M., I. J. Rae, I. R. Mann, K. R. Murphy, and V. Amalraj (2009), Ground-based Pc5 ULF wave power: Solar wind speed and MLT dependence, *J. Atmos. Sol. Terr. Phys.*, *71*, 1082–1092, doi:10.1016/j.jastp.2008.12.004.

Paulikas, G., and J. Blake (1976), Modulation of trapped energetic electrons at 6.6 R by direction of interplanetary magnetic-field, *Geophys. Res. Lett.*, *3*, 277–280, doi:10.1029/GL003i005p00277.

Paulikas, G. A., and J. B. Blake (1979), Effects of the solar wind on magnetospheric dynamics: Energetic electrons at the synchronous orbit, in *Quantitative Modeling of Magnetospheric Processes, Geophys. Monogr. Ser.*, vol. 21, edited by W. P. Olson, pp. 180–202, AGU, Washington, D. C., doi:10.1029/GM021p0180.

Plaschke, F., K.-H. Glassmeier, O. D. Constantinescu, I. R. Mann, D. K. Milling, U. Motschmann, and I. J. Rae (2008), Statistical analysis of ground based magnetic field measurements with the field line resonance detector, *Ann. Geophys.*, *26*, 3477–3489, doi:10.5194/angeo-26-3477-2008.

Plaschke, F., K.-H. Glassmeier, H. U. Auster, O. D. Constantinescu, W. Magnes, V. Angelopoulos, D. G. Sibeck, and J. P. McFadden (2009), Standing Alfvén waves at the magnetopause, *Geophys. Res. Lett.*, *36*, L02104, doi:10.1029/2008GL036411.

Posch, J., M. Engebretson, V. Pilipenko, W. Hughes, C. Russell, and L. Lanzerotti (2003), Characterizing the long-period ULF response to magnetic storms, *J. Geophys. Res.*, *108*(A1), 1029, doi:10.1029/2002JA009386.

Rae, I. J., et al. (2005), Evolution and characteristics of global Pc5 ULF waves during a high solar wind speed interval, *J. Geophys. Res.*, *110*, A12211, doi:10.1029/2005JA011007.

Rae, I. J., C. E. J. Watt, F. R. Fenrich, I. R. Mann, L. G. Ozeke, and A. Kale (2007), Energy deposition in the ionosphere through a global field line resonance, *Ann. Geophys.*, *25*, 2529–2539, doi:10.5194/angeo-25-2529-2007.

Reeves, G. D., S. K. Morley, R. H. W. Friedel, M. G. Henderson, T. E. Cayton, G. Cunningham, J. B. Blake, R. A. Christensen, and D. Thomsen (2011), On the relationship between relativistic electron flux and solar wind velocity: Paulikas and Blake revisited, *J. Geophys. Res.*, *116*, A02213, doi:10.1029/2010JA015735.

Rostoker, G., J. Samson, F. Creutzberg, T. Hughes, D. McDiarmid, A. Mcnamara, A. Jones, D. Wallis, and L. Cogger (1995), Canopus—A ground-based instrument array for remote-sensing the high-latitude ionosphere during the ISTP/GGS program, *Space Sci. Rev.*, *71*, 743–760, doi:10.1007/BF00751349.

Rostoker, G., S. Skone, and D. Baker (1998), On the origin of relativistic electrons in the magnetosphere associated with some geomagnetic storms, *Geophys. Res. Lett.*, *25*, 3701–3704, doi:10.1029/98GL02801.

Ruohoniemi, J., R. Greenwald, K. Baker, and J. Samson (1991), HF radar observations of Pc-5 field line resonances in the midnight/early morning MLT sector, *J. Geophys. Res.*, *96*, 15,697–15,710, doi:10.1029/91JA00795.

Samson, J., J. Jacobs, and G. Rostoker (1971), Latitude-dependent characteristics of long-period geomagnetic micropulsations, *J. Geophys. Res.*, *76*, 3675–3683, doi:10.1029/JA076i016p03675.

Samson, J., B. Harrold, J. Ruohoniemi, R. Greenwald, and A. Walker (1992), Field line resonances associated with MHD wave-guides in the magnetosphere, *Geophys. Res. Lett.*, *19*, 441–444, doi:10.1029/92GL00116.

Sarris, T. E., et al. (2009), Characterization of ULF pulsations by THEMIS, *Geophys. Res. Lett.*, *36*, L04104, doi:10.1029/2008GL036732.

Singer, H., C. Russell, M. Kivelson, E. Greenstadt, and J. Olson (1977), Evidence for control of Pc 3,4 magnetic pulsations by solar-wind velocity, *Geophys. Res. Lett.*, *4*, 377–379, doi:10.1029/GL004i009p00377.

Southwood, D. J. (1974), Some features of field line resonances in magnetosphere, *Planet. Space Sci.*, *22*, 483–491, doi:10.1016/0032-0633(74)90078-6.

Takahashi, K., R. E. Denton, and H. J. Singer (2010), Solar cycle variation of geosynchronous plasma mass density derived from the frequency of standing Alfvén waves, *J. Geophys. Res.*, *115*, A07207, doi:10.1029/2009JA015243.

Tamao, T. (1965), Transmission and coupling resonance of hydromagnetic disturbances in the non-uniform Earth's magnetosphere, *Sci. Rep. Tohoku Univ. Ser.*, *5*, 43–72.

Villante, U., P. Francia, and S. Lepidi (2001), Pc5 geomagnetic field fluctuations at discrete frequencies at a low latitude station, *Ann. Geophys.*, *19*, 321–325, doi:10.5194/angeo-19-321-2001.

Walker, A., J. Ruohoniemi, K. Baker, R. Greenwald, and J. Samson (1992), Spatial and temporal behavior of ULF pulsations observed by the Goose Bay HF radar, *J. Geophys. Res.*, *97*, 12,187–12,202, doi:10.1029/92JA00329.

Weatherwax, A., T. Rosenberg, L. Lanzerotti, C. Maclennan, H. Frey, and S. Mende (2000), The distention of the magnetosphere on May 11, 1999: High latitude Antarctic observations and comparisons with low latitude magnetic and geopotential data, *Geophys. Res. Lett.*, *27*, 4029–4032, doi:10.1029/2000GL000090.

Yeoman, T., D. Milling, and D. Orr (1990), Pi2 pulsation polarization patterns on the U.K. sub-auroral magnetometer network (SAMNET), *Planet. Space Sci.*, *38*, 589–602, doi:10.1016/0032-0633(90)90065-X.

Yumoto, K., T. Saito, and T. Sakurai (1983), Local time asymmetry in the characteristics of Pc 5 magnetic pulsations, *Planet. Space Sci.*, *31*, 459, doi:10.1016/0032-0633(83)90158-7.

Ziesolleck, C., and D. McDiarmid (1994), Auroral latitude Pc5 field line resonances: Quantized frequencies, spatial characteristics, and diurnal variation, *J. Geophys. Res.*, *99*, 5817–5830, doi:10.1029/93JA02903.

A. A. Chan, Department of Physics and Astronomy, Rice University, MS 108, 6100 Main St., Houston, TX 77005-1892, USA.

S. R. Elkington, Laboratory for Atmospheric and Space Physics, University of Colorado, 1234 Innovation Dr., Boulder, CO 80303, USA.

F. Honary, Department of Physics, University of Lancaster, Lancaster LA1 4YB, UK.

I. R. Mann, D. K. Milling, K. R. Murphy, L. G. Ozeke, and I. J. Rae, Department of Physics, University of Alberta, Edmonton, AB T6G 2G7, Canada. (jonathan.rae@ualberta.ca)